Thin Solid Films 582 (2015) 323–327

Contents lists available at ScienceDirect

Thin Solid Films

journal homepage: www.elsevier.com/locate/tsf

The structural properties of CdS deposited by chemical bath deposition and pulsed direct current magnetron sputtering

F. Lisco [a,*], P.M. Kaminski [a], A. Abbas [a], K. Bass [a], J.W. Bowers [a], G. Claudio [a], M. Losurdo [b], J.M. Walls [a]

[a] Centre for Renewable Energy Systems Technology (CREST), School of Electronic, Electrical and Systems Engineering, Loughborough University, Leicestershire, LE11 3TU, UK
[b] Institute of Inorganic Methodologies and of Plasmas, IMIP-CNR, via Orabona 4, 70126 Bari, Italy

ARTICLE INFO

Available online 28 November 2014

Keywords:
Pulsed direct-current magnetron sputtering
Chemical bath deposition
Cadmium sulphide
Thin films
Film uniformity
Pinhole free films
Void-free films

ABSTRACT

Cadmium sulphide (CdS) thin films were deposited by two different processes, chemical bath deposition (CBD), and pulsed DC magnetron sputtering (PDCMS) on fluorine doped-tin oxide coated glass to assess the potential advantages of the pulsed DC magnetron sputtering process. The structural, optical and morphological properties of films obtained by CBD and PDCMS were investigated using X-ray photoelectron spectroscopy, X-ray diffraction, scanning and transmission electron microscopy, spectroscopic ellipsometry and UV–Vis spectrophotometry. The as-grown films were studied and comparisons were drawn between their morphology, uniformity, crystallinity, and the deposition rate of the process. The highest crystallinity is observed for sputtered CdS thin films. The absorption in the visible wavelength increased for PDCMS CdS thin films, due to the higher density of the films. The band gap measured for the as-grown CBD-CdS is 2.38 eV compared to 2.34 eV for PDCMS-CdS, confirming the higher density of the sputtered thin film. The higher deposition rate for PDCMS is a significant advantage of this technique which has potential use for high rate and low cost manufacturing.

1. Introduction

Cadmium sulphide (CdS) is an important II–VI compound semiconductor material with applications in several heterojunction photovoltaic systems including cadmium telluride (CdTe), copper indium diselenide/sulphide and copper indium gallium diselenide/sulphide (CIGS) solar cells [1]. It has also applications in various electro-optic and infrared devices [2]. There are several deposition techniques used for the deposition of thin film CdS including RF sputtering [3,4], chemical bath deposition (CBD) [5], thermal evaporation [6], chemical vapour deposition [7], close space sublimation (CSS) [8], molecular beam epitaxy [9] and spray pyrolysis [10]. Each deposition process produces different structural, electrical and optical properties of the CdS thin films. In most heterojunction devices, high efficiency cells utilise a CdS window layer [11,12]. For example, First Solar has reported CdS deposited high-rate vapour transport deposition (HRVTD) [13]. A 14.2% efficient thin film CdTe solar cell with CdS deposited by CSS has been reported [14]. Use of RF sputtered CdS in CdTe solar cells resulted in an efficiency of 15.8% [15,16]. Interestingly, an efficiency of 21.7% has been reported for CIGS devices with CdS layers grown by CBD [17].

We have developed a process using pulsed DC magnetron sputtering (PDCMS) [18] to sputter thin films of CdS in highly stable process conditions. In this paper, we report on the differences in the properties of CBD and PDCMS deposited CdS thin films. The major advantage of the PDCMS process is that it produces high deposition rates which are much higher than those obtained using RF sputtering [19]. This makes the use of pulsed DC sputtering suitable for high throughput solar module manufacturing [18]. We also find that the energetics of the pulsed DC process produce favourable thin film properties. In addition, the use of pulsed DC power supplies avoids the need for complex matching circuits necessary when using radio frequency power supplies.

2. Experimental details

Transparent electrically conducting (TEC 10) glass supplied by NSG-Pilkington (http://www.pilkington.com/) was used as the substrate (superstrate) material. The substrates were cleaned in a two-step ultrasonic bath process followed by a plasma surface treatment prior to the CdS film growth [20]. CdS thin films of ~100 nm thickness were deposited by pulsed DC magnetron sputtering in a 'PV Solar' magnetron sputtering system (Power Vision Ltd., Crewe UK); details of the system have been provided elsewhere [18]. The deposition conditions were set using the following process parameters: 10 sccm of Ar gas flow, 500 W, 150 kHz, 2 s (ramping time), 2.5 μs (reverse time).

Thin films of CdS of ~100 nm thickness were deposited by chemical bath deposition (CBD); the reaction occurred in a beaker immersed in a water jacket to ensure constant temperature (70 °C). The bath solution consisted of 200 ml of de-ionised water, 15 ml of $Cd(CH_3COO)_2$ 0.01 M,

* Corresponding author. Tel.: +44 1509635351.
E-mail address: F.Lisco@lboro.ac.uk (F. Lisco).

http://dx.doi.org/10.1016/j.tsf.2014.11.062

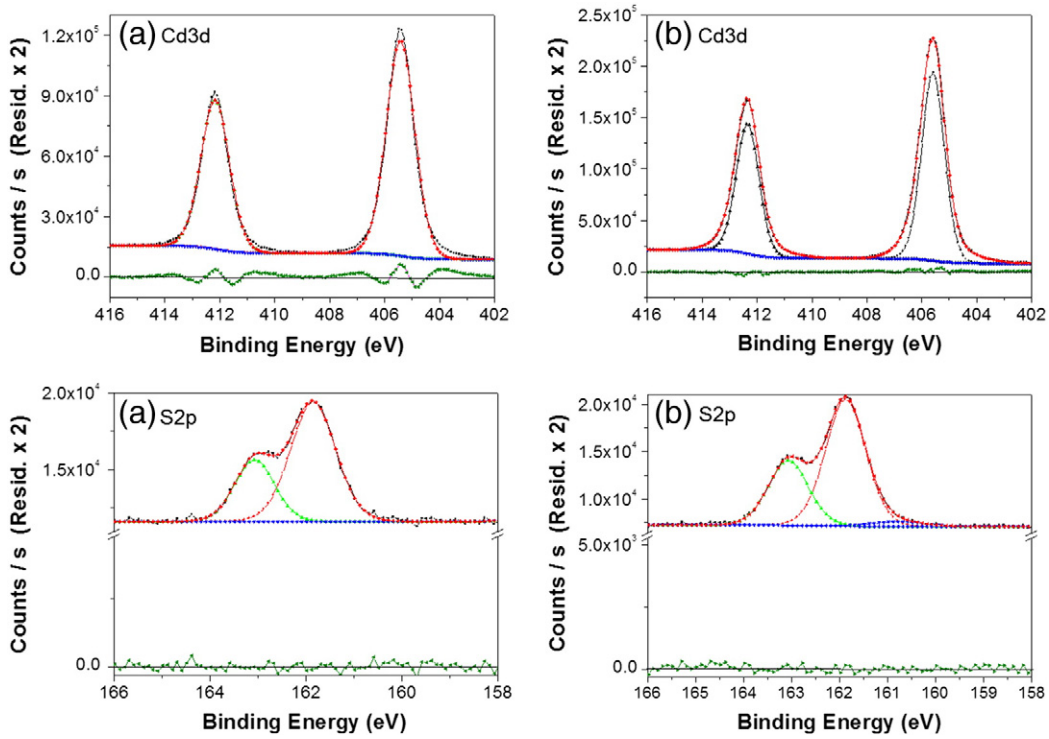

Fig. 1. The XPS spectra measured for pulsed DC and chemical bath deposited CdS films, were not affected by the deposition conditions, showing photoelectron core levels of (a) $Cd3d_{5/2}$ and $Cd3d_{3/2}$ and S2p for CdS thin films deposited at 10 sccm Ar, 500 W and 150 kHz and (b) $Cd3d_{5/2}$ and $Cd3d_{3/2}$ and S2p for CdS thin films deposited by chemical bath. For $Cd3d_{5/2}$ and $Cd3d_{3/2}$, the fitting is achieved with a single Gaussian peak due to CdS and for S2p the fitting shows the splitting $S2p_{3/2}$ and $S2p_{1/2}$. The green line at the bottom shows the error fitting function.

25 ml of NH_4OH 25% and 10 ml of $CS(NH_2)_2$, 0.1 M. An ultrasonic probe was immersed in the solution to accelerate the reaction kinetics [20].

The chemical composition, microstructure and optical properties of CdS thin films prepared by CBD and PCDMS were investigated and compared. The microstructure was studied with a high-resolution field emission gun scanning electron microscope (FEGSEM), Leo 1530 VP FEG-SEM, which provides the ability to visualise surface features of the material with nanometre resolution, operating at 5 kV. X-ray photoelectron spectroscopy (XPS) was used to obtain the surface chemical composition of the layers. The analysis was performed using a Thermo Scientific K-Alpha XPS surface analysis tool. An electron flood gun was used to reduce charging that would cause peak shifts to occur. An argon ion surface etch at 1 keV, for 30 s, was carried out prior to analysis to remove surface contamination. The X-ray source used was Al K_α radiation $h\nu = 1486.6$ eV with a beam diameter of 200 microns. The High Resolution Multiplex Scan was used to evaluate the chemical state(s) of each element through its core electron binding energies. Precise determination of binding energies was made through the use of curve fitting routines applied to the peaks in the multiplex scan and sensitivity factors were taken into account to determine elemental composition. A dual beam FEI Nova 600 Nanolab was employed to prepare the transmission electron microscopy (TEM) samples. A standard in situ lift off method was used to prepare cross-sectional samples through the coating into the glass substrate. A platinum over-layer was deposited to define the surface and homogenise the final thinning of the samples. TEM images were obtained using a Jeol JEM 2000FX operating at 200 kV, with an integrated camera above the phosphor screen to obtain digital images. The TEM technique provided morphological analysis of the grain structure of the sputtered and CBD CdS films on fluorine doped tin oxide (FTO) coated glass substrates (TEC 10). Scanning transmission electron microscopy (STEM) was carried out using a FEI Tecnai F20 (S) TEM, equipped with a silicon drift detector, in the common imaging mode for the STEM bright field imaging (BF). The X-ray diffraction analysis (XRD) was performed, using a Bruker D2 Phase bench-top XRD using copper X-rays with a 1.542 nm wavelength, to investigate the crystalline structure of the materials. Each sample was scanned using an angular range of 20–90 ° with a step size of 0.02 ° and a dwell time of 0.1 s. The transmission, reflection and energy gap (Eg) measurements were carried out using a spectrophotometer Varian Cary® UV–Vis 5000. The energy band gap E_g, was calculated by a graphic extrapolation by using the Tauc plot [21].

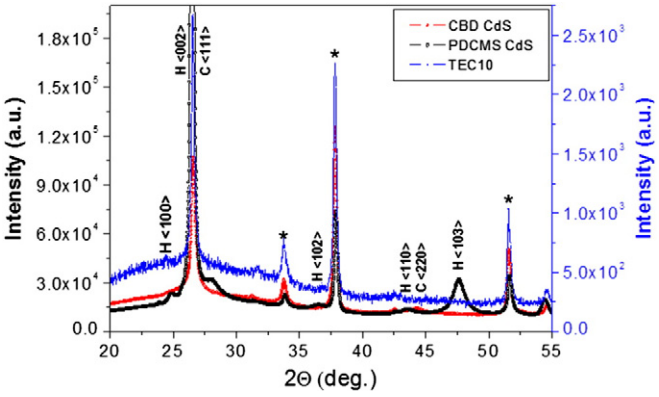

Fig. 2. XRD spectra of CBD and PDCMS CdS films. The peaks due to the hexagonal and cubic structure are indicated by H and C, respectively. The peaks due to the subtrate are indicated with *.

The optical properties of the thin films were measured using spectroscopic ellipsometry (SE) (Horiba, Jobin Yvon, UVISEL); which provided information about the thickness and refractive index (and uniformity) of the deposited films. The dispersion of the real and imaginary part of the refractive index was measured in a wavelength range between 248 nm and 2100 nm. The transparent electronic conductive (TEC 10) glass has a complex multilayer structure, being coated with successive layers of undoped SnO_2, SiO_2 and F-doped SnO_2, to achieve the desired sheet resistance. The optical properties of each component layer have been reported

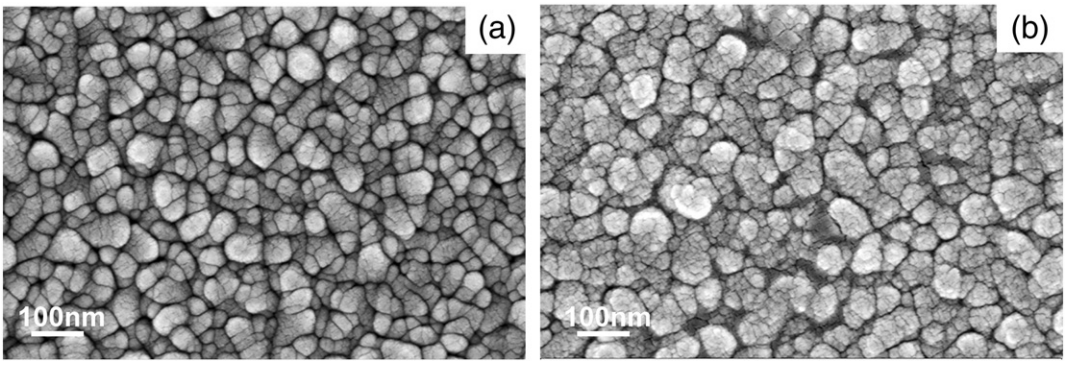

Fig. 3. SEM surface images of CdS films deposited by PDCMS (a) and CBD (b).

elsewhere [22]. The overall properties of the TEC 10 glass optical structure were measured by spectroscopic ellipsometry prior to CdS deposition. This data was then used as a fixed optical structure for the substrate in the ellipsometric model. The model consisted of a TEC-substrate/interface/CdS-film/surface-roughness/air structure to analyse SE data and derive the energy gap and refractive index of the CdS thin films. The CdS optical properties were obtained using a double Tauc Lorentz parameterisation [23]. The surface roughness was a Bruggeman Effective Medium Approximation (BEMA) [24] mixture of 50% CdS and 50% voids. The fit parameters were the Tauc parameters and layer thicknesses.

3. Results and discussion

Fig. 1(a) and (b) shows the XPS spectra of Cd3d and S2p photoelectron core levels measured for CdS films deposited by PDCMS sputtering and chemical bath deposited at 70 °C with $Cd(CH_3COO)_2$ 0.01 M, NH_4OH 25% and $CS(NH_2)_2$, 0.1 M, respectively. The binding energies of 405.8 eV and 412.3 eV for $Cd3d_{5/2}$ and $Cd3d_{3/2,}$ respectively, and 161.6 eV and 162.8 eV for $S2p_{3/2}$ and $S2p_{1/2}$ matched the theoretical values for CdS [25]. This indicates that the deposited CdS films are stoichiometric and no oxygen was incorporated into the films. This is also supported by fitting analysis, which showed only the CdS component.

The XRD analysis (see Fig. 2) is complicated by the coincidence of the TEC substrate and CdS film peaks; nevertheless, some analysis can be performed by examining the intensity of peaks and the different attenuation of the TEC peaks. Specifically, the very intense <002> reflection for the PDCMS CdS indicates the hexagonal structure with a preferential orientation <001>, whereas the CBD CdS films exhibit a cubic polycrystalline structure. The XRD analysis was referred to JCPDS database cards (http://www.icdd.com/).

Fig. 3 compares the surface morphologies of PDCMS (a) and CBD (b) deposited CdS thin films. The CBD deposited films have smaller crystallites compared to the PDCM sputtered films. Both show the onset of grain coalescence.

BF-STEM cross-sectional images of a 100 nm thick CdS film deposited on TEC10 glass by PDCMS and CBD are shown in Fig. 4(a) and (b), respectively. The grains expand through the thickness of the film deposited by PDCMS with a columnar structure (a) while small grainy crystallites grow through the thickness of CBD CdS film (b), consistent with the SEM images and XRD data. In both cases, the grains grow by following the structure of the substrate surface beneath (TEC10 glass) and voids are not observed at the interface.

Fig. 5 shows the derived optical properties, dispersion of the refractive index, *n*, and extinction coefficient, *k*, of the, CdS films deposited on TEC10 by PDCMS and CBD. The PDCMS CdS film shows a higher refractive index and a slightly higher absorption at 500 nm with sharper interband transition E_1 [23] (Fig. 5(b)). This can be explained by the increased grain size, increased density, and higher crystallinity observed for the films deposited by PDCMS compared to the CBD deposited CdS.

The transmittance of the thin films reaches a maximum of ~75% (this includes the effect of absorption in the TEC10 substrate) and decreases near the absorption edge at 500 nm, confirming the crystallinity of the CdS thin films (Fig. 6, inset). The PDCMS CdS has a lower transmission than the CBD deposited CdS, due to its higher optical density, in agreement with the ellipsometric analysis. Fig. 6 shows the band gap (E_g) determined from the Tauc plot. The PDCMS CdS has a band gap of 2.34 ± 0.01 eV compared to 2.38 ± 0.01 eV measured for the CBD CdS.

The deposition rate for CdS obtained using pulsed DC magnetron sputtering was 0.44 nm/s using only 500 W power on a six inch circular magnetron target. This rate is achieved on a 5 cm × 5 cm substrate located on a 180 mm diameter-rotating substrate carrier. The equivalent deposition rate for a static substrate is ~2.86 nm/s. The deposition rate using CBD is comparatively much slower. To deposit a 50 nm thick film of CdS required about 30 min and a thickness of 150 nm needed 1 h.

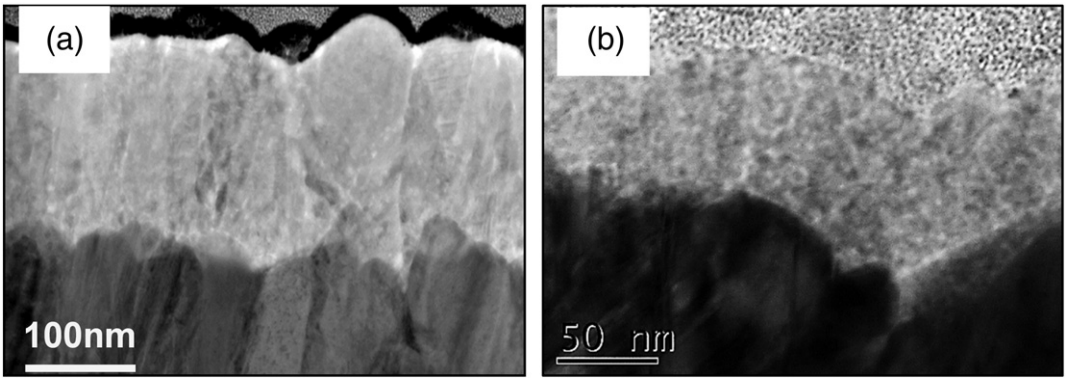

Fig. 4. TEM images of the sputtered CdS film (a) and CBD CdS film (b) both deposited on TEC10 coated glasses.

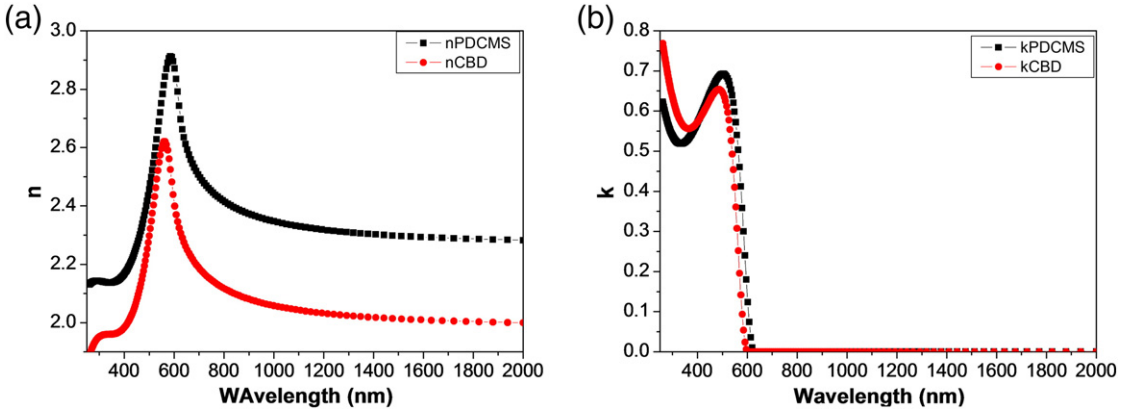

Fig. 5. Refractive index dispersion a of 100 nm CdS thin films, (a) real (n) and (b) imaginary part (k).

4. Conclusions

We have deposited and compared the properties of CdS thin films deposited by pulsed DC magnetron sputtering and chemical bath deposition. The pulsed DC magnetron sputtering process produced CdS thin films with the preferred hexagonal <001> oriented crystalline structure. TEM analysis shows evidence of columnar grain growth. Conversely, the CBD deposited films were polycrystalline with a cubic structure, showing small grainy crystallites throughout the thickness of the films. CBD deposited films exhibited comparatively poor thickness uniformity while the pulsed DC sputtered films were highly uniform. The spectroscopic ellipsometry analysis showed higher refractive index and slightly higher absorption at 500 nm for the PDCMS deposited CdS films, confirming the increased grain size, increased density, and higher crystallinity compared to the CBD CdS films. The films deposited by both techniques were pinhole and void-free, with an optical band gap of 2.34 ± 0.01 eV for the PDCMS deposited films and 2.38 ± 0.01 eV for CBD.

We have found that the deposition rate for CdS obtained using pulsed DC magnetron sputtering was 2.86 nm/s using only 500 W power on a six inch circular target. This is a high deposition rate and more than an order of magnitude faster than the chemical bath deposition technique. Moreover, we found that we could maintain process stability using 1.5 kW of power which produced a proportionate increase in deposition rate without affecting film quality. In comparison, deposition with RF sputtering is much slower. For example, deposition rates of 0.2 to 0.3 nm/s have been reported for powers in the range of 50 W to 250 W. This is approximately an order of magnitude slower than using pulsed DC power [18]. CBD deposition is also comparatively slow. In our case, it required 30 min to deposit a 50 nm thick film of CdS and 1 h for a 150 nm thick film. The comparative quality of the CdS thin films together with high rates of deposition shows that the pulsed DC magnetron sputtering process has the potential for application in high throughput and low cost manufacturing of solar modules.

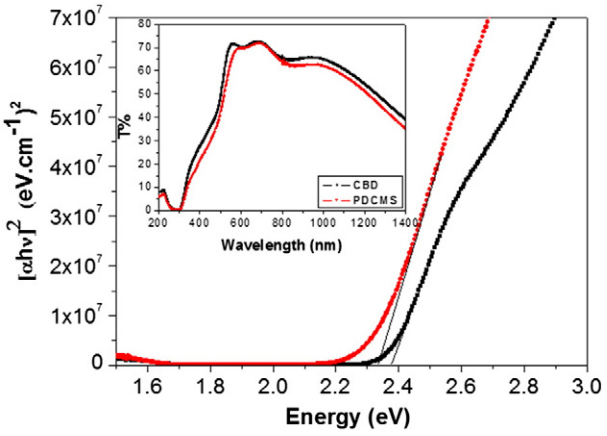

Fig. 6. Energy band gap, 2.34 ± 0.01 eV and 2.38 ± 0.01 eV for PDCMS and CBD thin films, respectively. Transmittance curve, as inset, for CdS films on TEC10 glass (the sample in the spectrophotometer is positioned letting the light pass through the glass/TCO/CdS layers).

Acknowledgements

The authors are grateful to the Engineering and Physical Science Research Council (EPSRC) (EP/J017361/1) for financial assistance under the Supergen SuperSolar Hub. They are also grateful to the Technology Strategy Board.

References

[1] I. Repins, S. Glynn, J. Duenow, T. Coutts, Required Materials Properties for High-Efficiency CIGS Modules, SPIE 7409, Thin Film Solar Technology, 74090 M (21 August 2009), NREL/CP-520-46235, 2009.
[2] M.A. Islam, M.S. Hossain, M.M. Aliyu, P. Chelvanathan, Q. Huda, M.R. Karim, K. Sopian, N. Amin, Comparison of structural and optical properties of CdS thin films grown by CSVT, CBD and sputtering techniques, Energy Procedia 33 (2013) 203.
[3] I. Mártil de LaPlaza, Structural and optical properties of rf-sputtered CdS thin films, Thin Solid Films 120 (1984) 31.
[4] A. Punnoose, M. Marafi, G. Prabu, F.E. Akkad, CdS thin films prepared by RF magnetron sputtering in Ar atmosphere, Phys. Status Solidi A 453 (2000) 453.
[5] F. Ouachtari, Influence of bath temperature, deposition time and S/Cd ratio on the structure, surface morphology, chemical composition and optical properties of CdS thin films elaborated by chemical bath deposition, J. Mod. Phys. 02 (2011) 1073.
[6] A. Ashour, N. El-Kadry, S.A. Mahmoud, On the electrical and optical properties of CdS films thermally deposited by a modified source, Thin Solid Films 269 (1995) 117.
[7] D. Barreca, A. Gasparotto, C. Maragno, E. Tondello, CVD of nanosized ZnS and CdS thin films from single-source precursors, J. Electrochem. Soc. 151 (2004) G428.
[8] D. Albin, Y. Yan, D. King, H. Moutinho, K. Jones, Processing Effects on Junction Interdiffusion in CdS/CdTe Polycrystalline Devices, NCPV Program Review Meeting 2000, 2000, p. 289.
[9] S. Petillon, A. Dinger, M. Gru, M. Hetterich, V. Kazukauskas, C. Klingshirn, J. Liang, B. Weise, V. Wagner, Molecular beam epitaxy of CdS/ZnSe heterostructures, J. Cryst. Growth 202 (1999) 453.
[10] A. Ashour, Physical properties of spray pyrolysed CdS thin films, Turk. J. Phys. 27 (2003) 551.
[11] P. Jackson, D. Hariskos, E. Lotter, S. Paetel, R. Wuerz, R. Menner, W. Wischmann, M. Powalla, New world record efficiency for Cu (In, Ga) Se 2 thin-film solar cells beyond 20%, Prog. Photovolt. Res. Appl. 19 (2011) 894.
[12] I. Repins, M.A. Contreras, B. Egaas, C. Dehart, J. Scharf, C.L. Perkins, 19.9%—efficient ZnO/CdS/CuInGaSe2 solar cell with 81.2% fill factor, Prog. Photovolt. Res. Appl. 16 (2008) 235.
[13] Rapid Deposition Technology Holds the Key for World's Largest Solar Manufacturer, http://www.nrel.gov/awards/2003_hrvtd.html2009 (Access date 2014).
[14] C.S. Ferekides, D. Marinskiy, S. Marinskaya, B. Tetali, D. Oman, D.L. Morel, CdS films prepared by the close space sublimation and their influence on CdTe/CdS solar cell performance, Photovoltaic Specialists Conference. Conference Record of the Twenty Fifth PVSC, May 13–17, 1996, IEEE, 1996, p. 751.
[15] P. Kelly, R. Arnell, Magnetron sputtering: a review of recent developments and applications, Vacuum 56 (2000) 159.
[16] R.D. Arnell, P.J. Kelly, Recent advances in magnetron sputtering, Surf. Coat. Technol. 112 (1999) 170.

[17] http://cleantechnica.com/2014/09/27/new-cigs-solar-cell-record-21-7-cigs-cell-conversion-efficiency-achieved-zsw/. New CIGS Solar Cell Record- ZSW, 2014. (Access date 2014).
[18] F. Lisco, P.M. Kaminski, A. Abbas, J.W. Bowers, G. Claudio, M. Losurdo, J.M. Walls, High Rate Deposition of thin film Cadmium Sulphide by Pulsed Direct Current magnetron sputtering, Thin Solid Films 541 (2015) 43–51.
[19] A.D. Compaan, C.N. Tabory, Y. Li, Z. Feng, A. Fischer, CdS/CdTe Solar Cells by RF Sputtering and by Laser Physical Vapor Deposition, Photovoltaic Specialists Conference. Conference. Conference Record of the Twenty Third IEEE, 1993, 1993, p. 394.
[20] F. Lisco, A. Abbas, B. Maniscalco, P.M. Kaminski, M. Losurdo, K. Bass, G. Claudio, J.M. Walls, Pinhole free thin film CdS deposited by chemical bath using a substrate reactive plasma treatment, J. Renew. Sustain. Energy 6 (2014) 011202.
[21] A. Rakhshani, Study of Urbach tail, bandgap energy and grain-boundary characteristics in CdS by modulated photocurrent spectroscopy, J. Phys. Condens. Matter 12 (2000) 4391.
[22] J. Chen, Spectroscopic Ellipsometry Studies of II–VI Semiconductor Materials and Solar Cells(PhD thesis) The University of Toledo, 2010.
[23] H. Fujiwara, Spectroscopic Ellipsometry: Principles and Applications, 1st edition Wiley, 2007.
[24] D. Gonçalves, E. Irene, Fundamentals and applications of spectroscopic ellipsometry, Quím. Nova 25 (2002) 794.
[25] D.A. Mazón-Montijo, M. Sotelo-Lerma, L. Rodríguez-Fernández, L. Huerta, AFM, XPS and RBS studies of the growth process of CdS thin films on ITO/glass substrates deposited using an ammonia-free chemical process, Appl. Surf. Sci. 256 (2010) 4280.